Ultrafast Shifted-Core Coaxial Nano-Emitter

UT Dallas Author(s):

Xi Li
Qing Gu

Citation:

Li, Xi, and Qing Gu. 2018. "Ultrafast shifted-core coaxial nano-emitter." Optics Express 26: 15177-15185, doi:10.1364/OE.26.015177

Research Article | Vol. 26, No. 12 | 11 Jun 2018 | OPTICS EXPRESS 15177
Optics EXPRESS

Ultrafast shifted-core coaxial nano-emitter

XI LI AND QING GU*

Department of Electrical and Computer Engineering, The University of Texas at Dallas, Richardson, TX 75080, USA
*qing.gu@utdallas.edu

Abstract: We present an ultrafast nanoscale light source utilizing a shifted-core coaxial nano-cavity, with a footprint of merely one-third of its emission wavelength in all three dimensions at telecommunication wavelengths. We show that, by shifting the metallic core off center of the coaxial structure, the effective mode volume of the cavity can be as small as $0.0078 \times (\lambda_0/n_a)^3$, resulting in a Purcell factor over 390 and a modulation bandwidth exceeding 60GHz. We further show that the evolution trend of the cavity Q factor as a function of core-shifting distance can be engineered by choosing proper substrate material. Compared to its symmetric counterpart, this shifted-core coaxial nano-cavity features not only higher Q factor, Purcell factor, and modulation bandwidth but also an improved emission directivity that is essential in its coupling with other on-chip components. The proposed nano-emitter also features robust single mode operation over the entire core-shifting range, resulting in a near-unity spontaneous emission factor. Therefore, this device can be a good candidate for low power optical interconnect applications.

OCIS codes: (140.3948) Microcavity devices; (230.6080) Sources; (320.7080) Ultrafast devices; (250.5403) Plasmonics.

References and links

1. D. A. B. Miller, "Attojoule optoelectronics for low-energy information processing and communications," J. Lightwave Technol. **35**(3), 346–396 (2017).
2. K. Liu, N. Li, D. K. Sadana, and V. J. Sorger, "Integrated nanocavity plasmon light sources for on-chip optical interconnects," ACS Photonics **3**(2), 233–242 (2016).
3. M. T. Hill, Y.-S. Oei, B. Smalbrugge, Y. Zhu, T. de Vries, P. J. van Veldhoven, F. W. M. van Otten, T. J. Eijkemans, J. P. Turkiewicz, H. de Waardt, E. J. Geluk, S.-H. Kwon, Y.-H. Lee, R. Nötzel, and M. K. Smit, "Lasing in metallic-coated nanocavities," Nat. Photonics **1**(10), 589–594 (2007).
4. M. P. Nezhad, A. Simic, O. Bondarenko, B. Slutsky, A. Mizrahi, L. Feng, V. Lomakin, and Y. Fainman, "Room-temperature subwavelength metallo-dielectric lasers," Nat. Photonics **4**(6), 395–399 (2010).
5. K. Ding, Z. C. Liu, L. J. Yin, M. T. Hill, M. J. H. Marell, P. J. Van Veldhoven, R. Nöetzel, and C. Z. Ning, "Room-temperature continuous wave lasing in deep-subwavelength metallic cavities under electrical injection," Phys. Rev. B. **85**, 041031 (2012).
6. M. Khajavikhan, A. Simic, M. Katz, J. H. Lee, B. Slutsky, A. Mizrahi, V. Lomakin, and Y. Fainman, "Thresholdless nanoscale coaxial lasers," Nature **482**(7384), 204–207 (2012).
7. E. K. Lau, A. Lakhani, R. S. Tucker, and M. C. Wu, "Enhanced modulation bandwidth of nanocavity light emitting devices," Opt. Express **17**(10), 7790–7799 (2009).
8. E. M. Purcell, "Spontaneous Emission Probabliities at Radio Frquencies," Phys. Rev. **69**, 674 (1946).
9. C.-Y. A. Ni and S. L. Chuang, "Theory of high-speed nanolasers and nano LEDs," Opt. Express **20**(15), 16450 (2012).
10. M. S. Eggleston and M. C. Wu, "Efficient coupling of an antenna-enhanced nanoLED into an integrated InP waveguide," Nano Lett. **15**(5), 3329–3333 (2015).
11. S. A. Fortuna, C. Heidelberger, K. Messer, K. Han, E. A. Fitzgerald, E. Yablonovitch, and M. C. Wu, "Optical antenna enhanced spontaneous emission rate in electrically injected nanoscale III-V LED," in *Conf. Dig. - IEEE Int. Semicond. Laser Conf.* (2016), pp. 2–3.
12. T. Baba, M. Fujita, A. Sakai, M. Kihara, and R. Watanabe, "Lasing characteristics of GaInAsP-InP strained quantum-well microdisk injection lasers with diameter of 2-10 μm," IEEE Photonics Technol. Lett. **9**(7), 878–880 (1997).
13. M. K. Seo, K. Y. Jeong, J. K. Yang, Y. H. Lee, H. G. Park, and S. B. Kim, "Low threshold current single-cell hexapole mode photonic crystal laser," Appl. Phys. Lett. **90**(17), 171122 (2007).
14. M.-K. Kim, A. M. Lakhani, and M. C. Wu, "Efficient waveguide-coupling of metal-clad nanolaser cavities," Opt. Express **19**(23), 23504–23512 (2011).
15. M.-K. Kim, Z. Li, K. Huang, R. Going, M. C. Wu, and H. Choo, "Engineering of metal-clad optical nanocavity

#326563 https://doi.org/10.1364/OE.26.015177
Journal © 2018 Received 21 Mar 2018; revised 22 May 2018; accepted 22 May 2018; published 31 May 2018

Optics EXPRESS

to optimize coupling with integrated waveguides," Opt. Express **21**(22), 25796–25804 (2013).
16. Y.-H. Jin, B. J. Park, and M.-K. Kim, "Extreme field enhancement in nano-gap plasmonic cavity via 90% efficient coupling with silicon waveguide," Opt. Express **24**(22), 25540–25547 (2016).
17. B. Bahari, R. Tellez-Limon, and B. Kante, "Directive and enhanced spontaneous emission using shifted cubes nanoantenna," J. Appl. Phys. **120**(9), 093106 (2016).
18. D. A. Genov, R. F. Oulton, G. Bartal, and X. Zhang, "Anomalous spectral scaling of light emission rates in low-dimensional metallic nanostructures," Phys. Rev. B. **83**, 245312 (2011).
19. C. Sauvan, J. P. Hugonin, I. S. Maksymov, and P. Lalanne, "Theory of the spontaneous optical emission of nanosize photonic and plasmon resonators," Phys. Rev. Lett. **110**(23), 237401 (2013).
20. R. C. Ge, P. T. Kristensen, J. F. Young, and S. Hughes, "Quasinormal mode approach to modelling light-emission and propagation in nanoplasmonics," New J. Phys. **16**(11), 113048 (2014).
21. P. T. Kristensen and S. Hughes, "Modes and Mode Volumes of Leaky Optical Cavities and Plasmonic Nanoresonators," ACS Photonics **1**(1), 2–10 (2014).
22. Q. Zhang, G. Li, X. Liu, F. Qian, Y. Li, T. C. Sum, C. M. Lieber, and Q. Xiong, "A room temperature low-threshold ultraviolet plasmonic nanolaser," Nat. Commun. **5**(1), 4953 (2014).
23. Q. Gu, B. Slutsky, F. Vallini, J. S. T. Smalley, M. P. Nezhad, N. C. Frateschi, and Y. Fainman, "Purcell effect in sub-wavelength semiconductor lasers," Opt. Express **21**(13), 15603–15617 (2013).
24. L. Novotny and B. Hecht, *Principles of Nano-Optics* (Cambridge University Press, 2009).
25. N. Yu, J. Fan, Q. J. Wang, C. Pflügl, L. Diehl, T. Edamura, M. Yamanishi, H. Kan, and F. Capasso, "Small-divergence semiconductor lasers by plasmonic collimation," Nat. Photonics **2**(9), 564–570 (2008).
26. G. V. Naik, V. M. Shalaev, and A. Boltasseva, "Alternative plasmonic materials: Beyond gold and silver," Adv. Mater. **25**(24), 3264–3294 (2013).
27. K. Ding and C. Z. Ning, "Fabrication challenges of electrical injection metallic cavity semiconductor nanolasers," Semicond. Sci. Technol. **28**(12), 124002 (2013).
28. Q. Gu, J. Shane, F. Vallini, B. Wingad, J. S. T. Smalley, N. C. Frateschi, and Y. Fainman, "Amorphous Al_2O_3 shield for thermal management in electrically pumped metallo-dielectric nanolasers," IEEE J. Quantum Electron. **50**(7), 499–509 (2014).

1. Introduction

Because of the urging demand for high-speed intrachip and chip-to-chip communication, the research of replacing the narrow band electronic communication link with optical link has been very active over the last decade [1]. However, the required on-chip light sources for optical links still have several limiting factors that restrict their practical applications: (1) relatively large physical dimension due to the diffraction limit of light, (2) low power efficiency owing to small spontaneous emission factor β (the ratio between spontaneous emission into the lasing mode and spontaneous emission into all modes), and (3) slow modulation speed because of gain compression effects in lasers. As a result, light sources for network applications are often considered off-chip [2].

The main challenges in reducing the size of light sources are to reduce both the cavity and modal sizes below the diffraction limit in all three dimensions, and to have a fully scalable cavity as most modes are in the cut-off regime for ultra-small cavity sizes [3–6]. The first challenge can be addressed by using metallic cavities, which offer extraordinary mode confinement; the second challenge can be addressed by using a cut-off free coaxial cavity design that supports the transverse electromagnetic (TEM) mode. In fact, a unity-β coaxial nanolaser has been demonstrated by combining both approaches [6]. As far as modulation speed is concerned, stimulated emission based lasers are limited by gain compression, while conventional LEDs have low direct modulation speed (<1GHz) due to long spontaneous emission lifetime (~1ns) [7]. By utilizing the Purcell effect, one can effectively enhance the spontaneous emission rate by altering the local electromagnetic environment [8], it was therefore proposed that nano-LED is a suitable light source for ultrafast on-chip communication systems [7,9–11]. Generally, there are two methods to increase the spontaneous emission rate: (1) decreasing the effective mode volume V_{eff} by using metallic cavities [4,6]; (2) implementing high Q factor dielectric cavities, such as microdisk and photonic crystal resonators [12,13]. Because nano-LED operates in the sub-threshold regime, high Q factors are not desired. In addition, the footprint of an on-chip light source should be kept small enough to be integrable with other components on chip. Based on these considerations, we aim to design a cavity with minimal V_{eff} and moderate Q factor.

Optics EXPRESS

In this work, we design a shifted-core coaxial nano-emitter supporting the cut-off free quasi-TEM mode [6], for applications in high density photonic integration. In section 2, we demonstrate that the shifted-core coaxial structure effectively squeezes the mode horizontally to the narrow gap between the metallic core and metallic shell, thus creating a hot spot in its near field [14–17]. Additionally, the cavity exhibits anomalous mode confinement behavior with increasing wavelength because of this strong mode confinement in the near-IR regime [18]. Consequently, extremely small effective mode volume is achieved, which results in an increase of Purcell factor, defined as the ratio of spontaneous emission in a cavity to that in free space, from 19 in the un-shifted case to 394 at the optimal shifting distance. In section 3, we show that the ultrafast spontaneous emission process gives rise to a wide modulation bandwidth of 62GHz, making this nano-emitter a suitable light source in high-speed optical communication links. By carefully choosing the cavity geometrical parameters, single mode operation can be enforced over the entire core shifting range for typical III-V materials. This feature of single mode operation grants near-unity spontaneous emission factor β for energy efficient operation; meanwhile, the deep sub-wavelength cavity size is maintained. In section 4, we explore the correlation of cavity Q factor with refractive index of the substrate material and operation temperature. We find that the evolution trend of cavity Q factor can be engineered by selecting different substrate materials. Lastly, in section 5, we show that by increasing the core shifting distance, the far-field pattern is changed from omni-directional to bi-directional, which is desirable for its integration with other photonic components on chip. We believe this ultra-compact and ultrafast nano-emitter is a promising light-source candidate for photonic integrated circuits, and paves the way towards the development of fully on-chip optical communication systems.

2. Shifted-core coaxial nano-emitter design

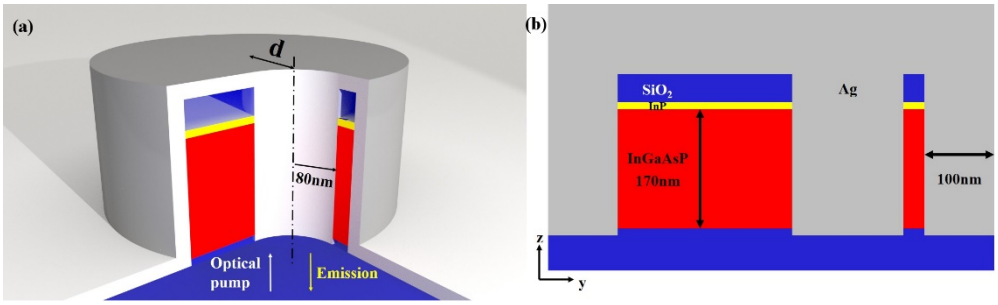

Fig. 1. Structure of the shifted-core coaxial nano-cavity. (a) 3D view. The SiO_2/InGaAsP/InP/SiO_2 layer stack forms a Fabry-Perot cavity in the vertical direction (InP layer functions as a protection layer). The Ag/InGaAsP/Ag structure forms a coaxial cavity in the horizontal direction. "d" denotes core-shifting distance in the xy-plane. (b) Cross sectional view of the un-shifted cavity.

The shifted-core coaxial nano-cavity is illustrated in Fig. 1(a). We use a III-V semiconductor gain material composed of five quantum wells of $In_{x=0.56}Ga_{1-x}As_{y=0.938}P_{1-y}$(10nm thick)/ $In_{x=0.734}Ga_{1-x}As_{y=0.57}P_{1-y}$ (20nm thick), of which the gain spectrum spans from 1.26μm to 1.59μm at room temperature (295K) [6]. We perform a parametric study of the nano-cavity to ensure that only the quasi-TEM mode is supported in the entire gain spectrum of InGaAsP quantum wells for a core shifting distance ranging from 0 to 110nm. In the un-shifted case, the InGaAsP ring structure has a uniform thickness of 140nm and a height of 170nm. The 10nm InP layer on top of InGaAsP quantum wells functions as a protection layer, resulting in a total III-V material height of 180nm. With the existence of high refractive index contrast between SiO_2 and III-V materials, the 40nm SiO_2 upper plug and 10nm SiO_2 lower plug help to form a Febry-Perot cavity in the vertical direction, while the metal-dielectric-metal structure forms a coaxial cavity in the horizontal direction. Therefore, the optical mode is confined in all three

Optics EXPRESS

dimensions. The above geometrical parameters result in a device footprint of 640 × 640 × 330nm^3.

To obtain the resonance wavelengths and quality factors of different modes in the nano-cavity, we perform eigenfrequency study using the wave optics module in COMSOL 5.3 (a commercially available FEM software). Figure 2(a) shows that, as the metallic core is shifted off center (increasing core shifting distance d), the Q factor increases while the resonance wavelength red shifts. With the increase in resonance wavelength, we may expect the mode to be less confined and eventually extinguished in the cavity. However, unlike the weakly confined 1D plasmonic mode, the strongly confined 2D quasi-TEM plasmonic mode under consideration actually exhibits an anomalous spectral scaling of light due to the tight electromagnetic field confinement [18]. This unique feature of the system greatly contributes to the reduction of the effective mode volume.

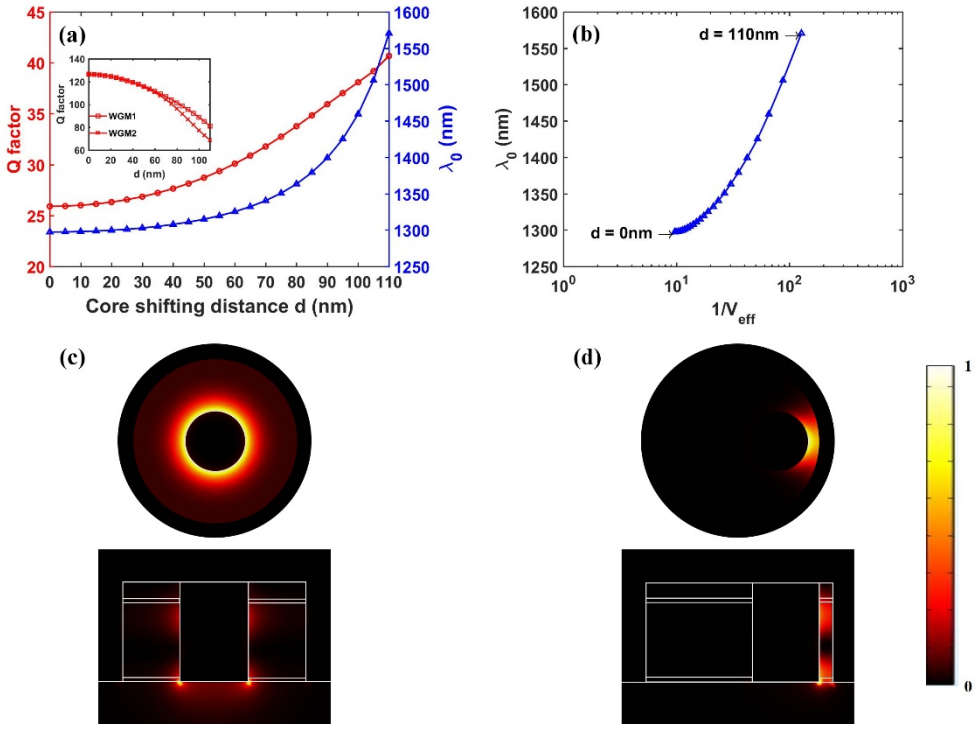

Fig. 2. Properties of the shifted core coaxial nano-cavity for different core shifting distance d (quasi-TEM mode). (a) Evolution of freespace resonance wavelength and quality factors. Inset: evolution of quality factors of whispering gallery mode (WGM1 and WGM2). (b) Anomalous spectral scaling of light. (c) yz-plane mode profile ($|E|^2$) at d = 0nm. (d) yz-plane mode profile ($|E|^2$) at d = 110nm.

As the mode confinement of this nano-cavity is larger than 0.5 in the entire core-shifting distance range and the field decays fast outside of the cavity, we can approximate this quasi-TEM mode as a normal mode. Therefore, we use a conventional effective mode volume formula to calculate the effective mode volume with good accuracy instead of using the generalized effective mode volume formula developed for quasi-normal mode [19–21]. A cavity's effective mode volume is defined as [22]:

Optics EXPRESS

$$V_{\text{eff}} = \frac{\Sigma_\alpha \int_{V_\alpha} W(\mathbf{r}_\alpha) d^3\mathbf{r}_\alpha}{\max(W(\mathbf{r}))} = \frac{\Sigma_\alpha \int_{V_\alpha} d^3\mathbf{r}_\alpha \left(\varepsilon_{g,\alpha}(\mathbf{r}_\alpha) |\mathbf{E}_\alpha(\mathbf{r}_\alpha)|^2 + \mu_\alpha(\mathbf{r}_\alpha) |\mathbf{H}_\alpha(\mathbf{r}_\alpha)|^2 \right)}{\max\left(\varepsilon_g(\mathbf{r}) |\mathbf{E}(\mathbf{r})|^2 + \mu(\mathbf{r}) |\mathbf{H}(\mathbf{r})|^2 \right)}. \quad (1)$$

Where α represents different domains for different materials in the system, and $\varepsilon_g = \frac{\partial[\omega \varepsilon_r(\mathbf{r},\omega)]}{\partial \omega}$ is the group permittivity of the material. The anomalous spectral scaling and the decrease in V_{eff} are shown in Fig. 2(b): when the metallic core shifts up to 110nm, the effective mode volume is reduced by more than one order of magnitude compared to the un-shifted case. The maximum shifting distance of 110nm is determined by the corresponding resonance wavelength limit set forth by the edge of the InGaAsP gain spectrum.

By shifting the metal core, the mode is horizontally squeezed into the narrow gap between the metal core and shell, as shown in Figs. 2(c) and 2(d), which significantly increases the local confinement of the electromagnetic field energy. Because of such tight mode confinement, the effective mode volume can be decreased below 0.01 (normalized to the cubic of wavelength in freespace) which corresponds to a Purcell factor F_p above 390 in Fig. 3(a). For low Q plasmonic cavities, the Purcell factor is defined as [3,8,23]:

$$F_p = \frac{3}{4\pi^2} \left(\frac{\lambda_c}{n_a} \right)^3 \left(\frac{Q}{V_{eff}} \right). \quad (2)$$

For photonic-mode nano-cavities such as the metallo-dielectric cavity, because the mode does not overlap with the electrically absorptive materials much, the electric energy and magnetic energy are almost identical as their energies are exchanged over an oscillation period $2\pi/\omega_0$. However, for the plasmonic-mode nano-cavity discussed here, because the field antinode is located at the metal-dielectric interface, the evanescent electric field exponentially decays in metal. As a result, energy not only builds up but also transfers into metal and dissipates as heat [24]. Therefore, we need to consider unequal electric and magnetic energies, and use the total electromagnetic energy in the effective mode volume and Purcell factor calculation. Figure 3(a) shows that falsely using the electric energy results in an over-estimated Purcell factor (a ratio of 1.4 in the most over-estimated case).

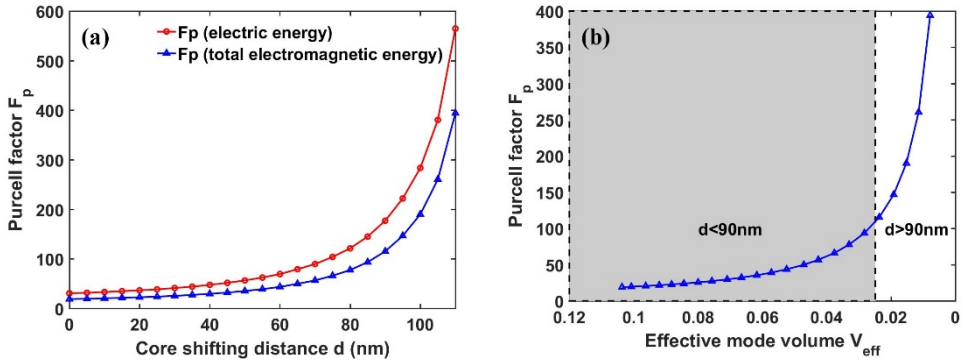

Fig. 3. Properties of the shifted core coaxial nano-cavity for different core shifting distance d. (a) Purcell factor comparison between calculation using electric energy and total electromagnetic energy. (b) Purcell factor's dependence on effective mode volume.

Optics EXPRESS

While increasing Q factor and decreasing V_{eff} are both viable methods to increase the Purcell factor, Fig. 3(b) shows that the increase of Purcell factor mainly stems from the decrease of the effective mode volume. Above 90nm core shifting distance, F_p increases rapidly in an exponential fashion with respect to V_{eff}. These results validate the effectiveness of decreasing V_{eff} as an efficient way to increase the spontaneous emission rate. Compared to the un-shifted case, the normalized effective mode volume is suppressed more than 10 times at maximum shifting distance, due to the strong electromagnetic field confinement to the small gap between the metallic walls in Fig. 2(b). As the quasi-TEM mode is cut-off free and less sensitive to the deformation of the symmetric coaxial structure, the Q factor changes gradually with respect to the core shifting distance d in Fig. 2(a). Combining the effect of effective mode volume and quality factor, the Purcell factor increases from 19 in the un-shifted case to 394 at maximal shifting distance (Fig. 3). Lastly, we note that throughout the entire shifting range, a near-unity β-factor is maintained by enforcing the quasi-TEM mode to always be the only resonance mode in the gain spectrum of InGaAsP quantum well.

3. Modulation bandwidth

Because of the relatively low Q factor of this nano-emitter, we can assume that the spontaneous emission process dominates the radiative emission over the entire core shifting range at room temperature. The simplified modulation bandwidth formula for nano-LEDs writes as [7]:

$$f_{3dB,\max} \approx \frac{1}{2\pi}\frac{1}{\sqrt{\tau_p^{\,2}+\tau_{sp}^{\,2}}}. \tag{3}$$

The modulation bandwidth's dependence on core shifting distance is depicted in Fig. 4(a). In Eq. (3), both the photon lifetime τ_p and the spontaneous emission lifetime τ_{sp} limit the modulation bandwidth. τ_p and τ_{sp} as a function of core shifting distance is plotted in Fig. 4(b). Although photon lifetime shows an increasing trend (inset of Fig. 4(b)) like the Q factor evolution, its effect on modulation bandwidth is minimal because of its relatively small absolute value. In the sub-threshold regime, the slow spontaneous emission is the dominant process.

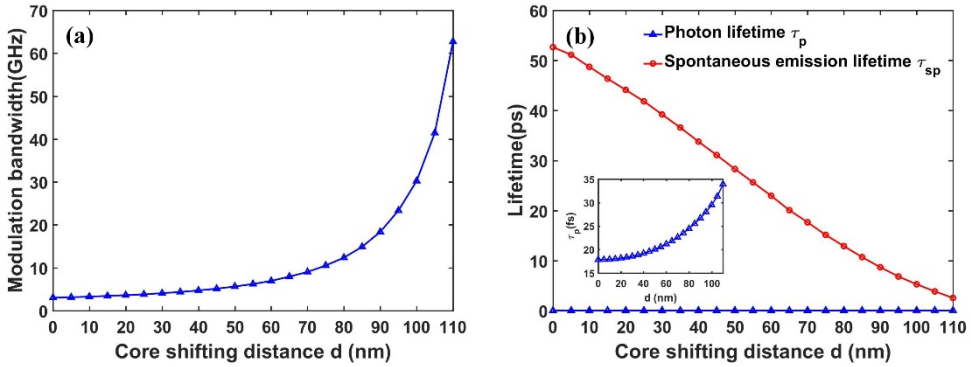

Fig. 4. Properties of the shifted core coaxial nano-cavity for different core shifting distance d. (a) Modulation bandwidth. (b) Photon lifetime and spontaneous emission lifetime. Inset: expanded figure of photon lifetime.

By shifting the metal core, the Purcell factor can reach as high as 394, indicating a significantly shortened spontaneous emission lifetime. Thus, the modulation bandwidth can reach as high as 62GHz – about a 20-time improvement compared to the un-shifted case – which is also much faster than conventional lasers and LEDs.

Optics EXPRESS

4. Effects of substrate refractive index and operation temperature

In account of the increasing overlapping region of the quasi-TEM mode and metal when the metallic core shifts to one side of the cavity, the Q factor is generally expected to decrease. We showed in Fig. 2(a) that this is not the case for our cavity. In fact, the evolution of Q factor as a function of core-shifting distance d can exhibit opposing trends in different material platforms. Figure 5(a) depicts the Q factor evolution for a range of substrate refractive indices, in which a decreasing trend for $n_{substrate} < 1.1$ and an increasing trend for $n_{substrate} > 1.3$ are observed. To study this atypical behavior, we analyze the loss channels in the system by calculating the energy distribution.

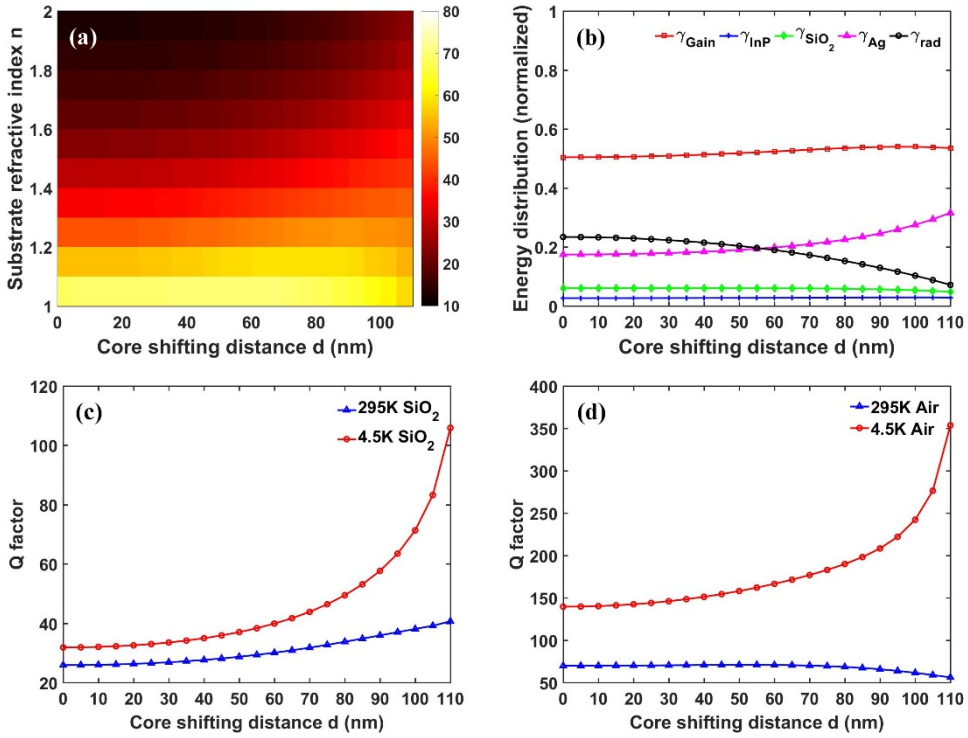

Fig. 5. (a) Q factor as a function of d and n (refractive index of cavity lower plug and substrate material) at 295K. (b) Normalized energy distribution as a function of d (SiO_2 as lower plug and substrate material). (c) Q factor at different temperatures for SiO_2 lower plug and substrate material; (d) Q factor at different temperatures for air plug and no substrate.

There exist two main loss terms in this cavity: (i) metal absorption loss (increases as the metal core shifting distance d increases); (ii) radiation loss (decreases as the core-shell gap diminishes or as the refractive index difference between the gain and substrate materials increases). In the case of SiO_2 lower plug (the layer of material underneath the gain medium) and substrate, for a given lower plug height, the metal absorption loss and radiation loss show opposing trends with respect to d in Fig. 5(b). As the radiation loss evolution is also affected by $n_{substrate}$, the competition between these two loss terms will therefore determine the Q factor of the cavity, which is a function of both d and n, as shown in Fig. 5(a). In the vertical direction, because the cavity supports a Fabry-Perot mode in which mode confinement results from total internal reflection, the radiation loss always increases when the refractive index of the cavity lower plug and substrate approaches that of the gain medium (refractive index of 3.4). If $n_{substrate}$ is low, the index contrast between the plug and gain will be strong. Therefore, the change of radiation loss with respect to d will be minimal, and metal absorption will be

Optics EXPRESS

the dominant term in determining the Q factor. This is the scenario for substrate $n_{substrate}<1.1$ (i.e. in the case of an air substrate). Under this circumstance, the Q factor remains almost unchanged at small d and then decreases at large d, as shown in Fig. 5(a). When $1.1< n_{substrate}<1.3$, there is an optimal core shifting distance d at which Q factor peaks. On the other hand, by increasing the refractive index of the lower plug and substrate, the index contrast between gain and lower plug becomes lower and the mode confinement in the vertical direction is weaker. In this case ($n_{substrate} > 1.3$), the Q factor as a function of d can have an increasing trend. A slice of Fig. 5(a) for $n_{substrate} = n_{SiO2} = 1.44$ is presented in Fig. 2(a). Common waveguide materials such as SiO_2, Al_2O_3 and Si_3N_4 all belong to the category of $n_{substrate} > 1.3$, and we utilize the increasing Q trend with d by using these materials. Recognizing the different slopes of Q factor evolution with different lower plug and substrate material, we can choose the dominant loss term and engineer the evolution of Q factor by appropriately choosing the substrate material.

Lastly, in Figs. 5(c) and 5(d), we examine the temperature effects on the cavity performance using two commonly used experimental condition, room temperature and 4.5K, with air substrate and SiO_2 substrate respectively. As the extinction coefficient of Ag at 4.5K is only 1% of that at room temperature, the Q factor increases with increasing d at 4.5K due to the smaller metal absorption loss for both SiO_2 and air substrates. Because of the negligible metal absorption loss at 4.5K, the radiation loss becomes the dominant loss term. Interestingly, Fig. 5(d) shows that, for air substrate, at room temperature and 4.5K, the Q factor evolutions exhibit opposing trends, as they follow the evolution of metal absorption loss and radiation loss respectively in Fig. 5(b). Therefore, active temperature tuning can be a method to dynamically change the evolution of Q factor, if desired.

5. Engineering far-field emission pattern

Because of the small aperture and omni-directional emission feature of the symmetric nano-coaxial cavity, only limited amount of power can be channeled into other on-chip components such as a waveguide. By shifting the metallic core of this cavity, the electric field is strongly localized in the gap between the core and shell, therefore, in the xy-plane the field perpendicular to the core-shifting direction is suppressed, and the far-field emission pattern changes from omni-directional in Fig. 6(a) to bi-directional (in-line with the metal core shifting direction, Fig. 6(b)). In Fig. 6(c), we also present the evolution of emission directivity as a function of core-shifting distance. Although out of the scope of this work, one can use metallic grating as plasmonic collimator to improve beam quality, as small aperture results in divergence of the beam [25].

In order to improve the coupling efficiency to waveguide for on-chip applications, bottom coupling can be used to couple the emission into a waveguide. However, as the coaxial nano-cavity supports the quasi-TEM mode, while a typical dielectric slab waveguide only supports TE or TM modes, the mode mismatch will result in a low coupling efficiency. One possible solution is to use a slot line plasmonic waveguide, in which two conductors are utilized for the waveguide to support the TEM mode. Concerning the conductive material to be used for the slot waveguide, novel metals such as silver or gold, as well as low loss aluminum doped zinc oxide (AZO) are potential candidates [26].

Optics EXPRESS

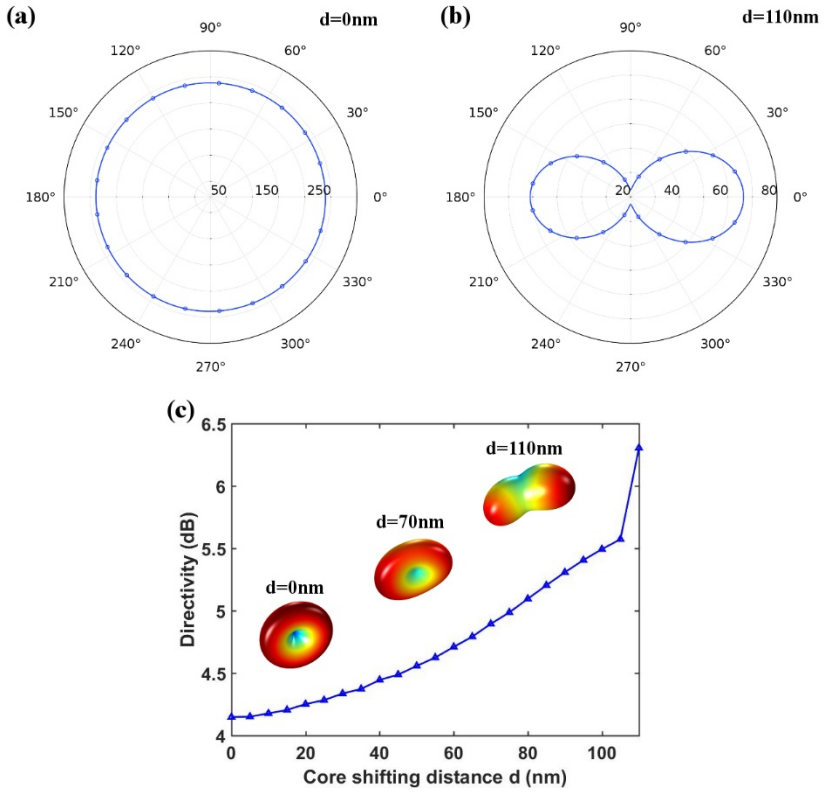

Fig. 6. Far-field emission pattern of the shifted core coaxial nano-cavity. (a) d = 0nm; (b) d = 110nm. Omni-directional emission can be changed to in-line bi-directional emission; (c) Evolution of emission directivity as a function of core-shifting distance d.

6. Discussions and conclusions

We have systematically studied a shifted-core coaxial nano-cavity. By controlling the metal core shifting distance, we can engineer the local field confinement. Through numerical simulation, we have demonstrated high Purcell factor and broad modulation bandwidth up to 394 and 62GHz, respectively. The effect of substrate refractive index and temperature has also been studied for the purpose of on-chip integration. Moreover, we prove that the cavity far-field pattern can be engineered by shifting the metallic core to increase emission directionality.

Future directions of this work include the experimental demonstration of optically pumped shifted-core coaxial nano-emitters, followed by the extension of the design to be fit for electrical injection, as electrically pumped laser/LED operation is the ultimate goal of optical sources for on chip communication applications [27,28]. In addition, studies of coupled shifted-core coaxial nano-cavities with different separation distances are of interest: with the mode strongly confined in the near vicinity of the gap, strong mode splitting of the bonding and anti-bonding modes can be expected. We believe this ultra-compact and ultrafast nano-cavity is a good candidate of light source for chip scale optical communications systems and is amenable to integration with other photonic components such as waveguides, amplifiers, modulators and detectors. In can also be a good platform to study the physics of coupled resonators.

Funding

UT Dallas faculty start-up fund.